INTERNATIONAL JOURNAL FOR NUMERICAL METHODS IN FLUIDS
Int. J. Numer. Meth. Fluids 2003; **42**:147–162 (DOI: 10.1002/fld.466)

Calculation of turbulent fluid flow and heat transfer in ducts by a full Reynolds stress model

Masoud Rokni and Bengt Sundén*,†

Division of Heat Transfer, Lund Institute of Technology, Box 118, 221 00 Lund, Sweden

SUMMARY

A computational method has been developed to predict the turbulent Reynolds stresses and turbulent heat fluxes in ducts by different turbulence models. The turbulent Reynolds stresses and other turbulent flow quantities are predicted with a full Reynolds stress model (RSM). The turbulent heat fluxes are modelled by a SED concept, the GGDH and the WET methods. Two wall functions are used, one for the velocity field and one for the temperature field. All the models are implemented for an arbitrary three-dimensional channel.

Fully developed condition is achieved by imposing cyclic boundary conditions in the main flow direction. The numerical approach is based on the finite volume technique with a non-staggered grid arrangement. The pressure–velocity coupling is handled by using the SIMPLEC-algorithm. The convective terms are treated by the van Leer scheme while the diffusive terms are handled by the central-difference scheme. The hybrid scheme is used for solving the ε equation.

The secondary flow generation using the RSM model is compared with a non-linear k–ε model (non-linear eddy viscosity model). The overall comparison between the models is presented in terms of the friction factor and Nusselt number. Copyright © 2003 John Wiley & Sons, Ltd.

KEY WORDS: Reynolds stress model; duct flow; non-linear k–ε model; turbulent flow

1. INTRODUCTION

Channels of various cross-sections occur frequently in compact heat exchangers and gas turbine cooling systems. Secondary motion of *Prandtl's second* kind takes place in non-circular straight ducts in the plane perpendicular to the main flow direction and is driven by the turbulence. These motions are of importance since they redistribute the kinetic energy, influence the axial velocity and thereby affect the wall shear stress and heat transfer. A linear k–ε model does not have the ability to predict secondary flows, but still it is one of the most popular models due to its simplicity and decent overall properties. Adding non-linear terms to the constitutive relation for the Reynolds stresses allows the model to predict more

*Correspondence to: B. Sundén, Division of Heat Transfer, Lund Institute of Technology, Box 118, 221 00 Lund, Sweden.
†E-mail: bengts@emvox2.vok.lth.se

Received September 2001
Revised 15 August 2002

reliable anisotropic normal stresses, and then secondary flows may be predicted without solving additional equations.

A differential Reynolds stress model (RSM) is able to predict secondary flows; however, the increased complexity of the model may cause stability problems together with a significant increase in computational effort. In RSM modelling, the expression for the pressure-strain tensor may be the most difficult part to model since it plays a critical role in a variety of turbulent flows of engineering interest and it involves unmeasurable correlations. Consequently, the development of RSMs to have a reliable predictive ability is essentially dependent on the proper modelling of the pressure-strain correlation. The pressure-strain redistribution consists of three parts, slow part, rapid part and the wall-reflection term which follows exactly from the Poisson equation for the pressure fluctuations (see, e.g. Reference [1]). The first two parts are the volume integrals of the two-point correlations, whereas the last part represents the surface integral and is effective only in the presence of a solid wall or an interphase surface.

The wall-reflection term is supposed to simulate the surface integral and has a net effect in the direction normal to a wall by damping the fluctuations only. Since this term includes normal distances to walls, the application of wall-reflection terms into a general complex geometry is an uncomfortable task and seems not to be practicable, even for a moderate complex geometry. For example, one can construct at any point of the flow along a right-angled corner, two directions normal to a wall. Therefore, it is desirable to propose a model for the pressure-strain without the need for wall-reflection terms or include their effects into the other parts (rapid term). A few such models have been proposed. For instance, Launder and Li [2] used a realizable cubic model for the rapid part and eliminated the wall-reflection terms. However, the pressure strain term which is used in this study and does not need any wall-reflection term, was presented by Speziale *et al.* [3], hereafter named as the SSG.

Several fundamental investigations concerning turbulent flow in square and rectangular ducts exist in the literature. Rokni and Sundén [4, 5] have successfully employed the non-linear k–ε model proposed by Speziale for predicting the flow and heat flux in straight and corrugated ducts with trapezoidal cross-sections. Non-circular ducts have not been explored widely. Demuren and Rodi [6] used algebraic expressions for the Reynolds stresses by refining the RSM of Launder *et al.* [7] to predict the secondary motions in square ducts. Mompean *et al.* [8] used several non-linear eddy viscosity models to predict the secondary flows in a square duct. Naimi and Gessner [9] and Myong and Kobayashi [10] studied also flow in a square duct without showing secondary motions vectors. Launder and Li [2] indicated how to eliminate the wall-topography (wall-reflection of the pressure-strain) from the RSM models and then the secondary flows in square and rectangular ducts. However, all these studies concerned ducts with orthogonal cross-sections (square and rectangular) and no study on 3D ducts with non-orthogonal cross-section is available in the open literature using RSM, as the literature survey of the authors showed.

This investigation concerns numerical calculation of turbulent forced convective heat transfer and fluid flow in straight ducts at fully developed conditions. In this paper the authors have developed a computational method to predict the turbulent Reynolds stresses and turbulent heat fluxes in ducts using a full differential Reynolds stress model (RSM). The results are compared with those predicted by the standard k–ε model and the non-linear k–ε model of Speziale [11]. The turbulent heat fluxes are modelled with the simple eddy diffusivity (SED)

concept, GGDH and WET methods in arbitrary three-dimensional channels. The combination of a RSM model for the fluid flow with GGDH and WET models for the heat fluxes has not been found in the literature and this is a unique feature of this paper.

One difficulty associated with turbulent convective heat transfer and fluid flow in ducts is obtaining satisfactory results for both friction factor and *Nu*-number, if wall functions are used. Usually, either friction factor or *Nu*-number can be predicted satisfactory, not both of them.

Although the RSM calculation procedure developed in this study does not need any normal wall distance for the Reynolds stresses but wall functions are used for the velocity and temperature fields. This implies that the limitation is the wall functions demanding that the y^+ adjacent to a solid wall should be greater than about 30. However, in many industrial applications the number of grid points used near a wall are few (due to limitation of cost and time) and the y^+ near the solid wall automatically are greater than about 30.

2. PROBLEM STATEMENT

Straight ducts with arbitrary cross-sections are considered in this investigation. Mean velocity distribution, turbulent quantities, friction factors and *Nu*-numbers are determined numerically for fully developed conditions. The secondary flow generation is also of major concern. The following assumptions are employed: steady state, no-slip at the wall and constant fluid properties.

Only one quarter of the ducts with square and rectangular cross-sections and only half of the duct with trapezoidal cross-section are considered by imposing symmetry conditions. A principle sketch of a duct is shown in Figure 1.

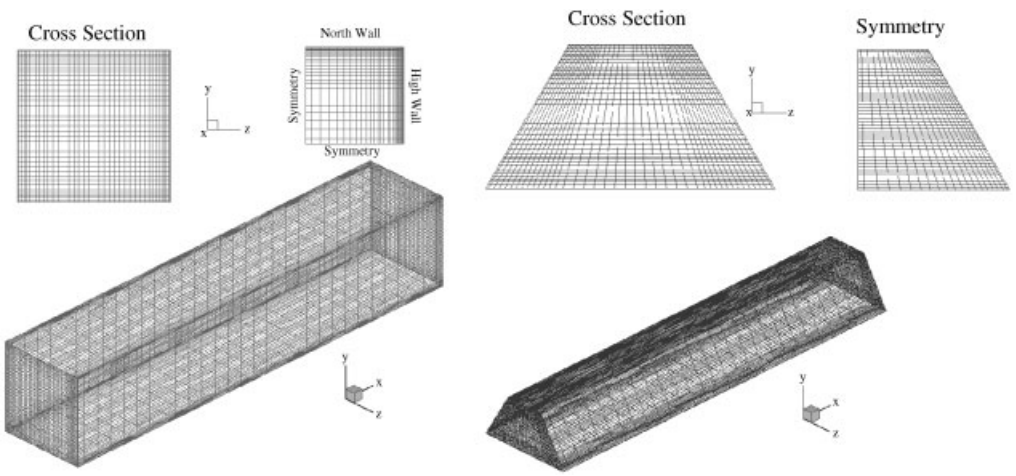

Figure 1. Ducts under consideration.

3. GOVERNING EQUATIONS

The governing equations are the continuity, momentum equations and energy equation at steady state.

$$\frac{\partial \rho}{\partial t} + \frac{\partial}{\partial x_j}(\rho U_j) = 0 \tag{1}$$

$$\frac{\partial(\rho U_i)}{\partial t} + \frac{\partial}{\partial x_j} + (\rho U_i U_j) = -\frac{\partial P}{\partial x_i} + \frac{\partial}{\partial x_j}\left[\mu\left(\frac{\partial U_i}{\partial x_j} + \frac{\partial U_j}{\partial x_i}\right)\right] + \frac{\partial}{\partial x_j}(-\rho\overline{u_i u_j}) \tag{2}$$

$$\frac{\partial(\rho T)}{\partial t} + \frac{\partial}{\partial x_j}(\rho U_j T) = \frac{\partial}{\partial x_j}\left[\frac{\mu}{Pr}\frac{\partial T}{\partial x_j}\right] + \frac{\partial}{\partial x_j}(-\rho\overline{u_j t}) \tag{3}$$

Fully developed periodic turbulent flows with constant fluid properties are considered. The turbulent stresses $(-\rho\overline{u_i u_j})$ and the turbulent heat fluxes $(\rho c_p \overline{u_j t})$ are modelled as described in the following sections.

3.1. *Full Reynolds stress modelling* (*RSM*)

The Reynolds stress tensor $(-\rho\overline{u_i u_j})$ is a solution of the transport equation as expressed below, (in Cartesian co-ordinate system)

$$\frac{\partial}{\partial t}(-\rho\overline{u_i u_j}) + \frac{\partial}{\partial x_k}(\rho U_k \overline{u_i u_j}) = P_{ij} + \Phi_{ij} - \varepsilon_{ij} + \frac{\partial}{\partial x_k}\left(\mu\frac{\partial \overline{u_i u_j}}{\partial x_k} - C_{ijk}\right) \tag{4}$$

where

$$P_{ij} = -\rho\left(\overline{u_i u_k}\frac{\partial U_j}{\partial x_k} + \overline{u_j u_k}\frac{\partial U_i}{\partial x_k}\right), \quad \Phi_{ij} = -\overline{p\left(\frac{\partial u_i}{\partial x_j} + \frac{\partial u_j}{\partial x_i}\right)} \tag{5}$$

$$\varepsilon_{ij} = 2\mu\frac{\partial u_i}{\partial x_k}\frac{\partial u_j}{\partial x_k}$$

$$C_{ijk} = \rho\overline{u_i u_j u_k} + \overline{p u_i}\delta_{jk} + \overline{p u_j}\delta_{ik} \tag{6}$$

are production, pressure-strain correlation, dissipation rate tensors and third-order diffusion correlation. Using the Kolmogorov assumption of local isotropy, the dissipation rate tensor can be expressed as

$$\varepsilon_{ij} = \frac{2}{3}\varepsilon\delta_{ij} \tag{7}$$

where ε is the scalar turbulent dissipation rate. Speziale *et al.* [3], hereafter named as the SSG model, presented the following expression for the pressure-strain tensor, which does not

need any wall reflection

$$\Phi_{ij} = -(C_1\rho\varepsilon + C_1^*\wp)b_{ij} + C_2\rho\varepsilon\left(b_{ik}b_{kj} - \frac{1}{3}b_{mn}b_{mn}\delta_{ij}\right) + \rho k S_{ij}(C_3 - C_3^*\Pi^{0.5}) + C_4\rho k\left(b_{ik}S_{jk} + b_{jk}S_{ik} - \frac{2}{3}b_{mn}S_{mn}\delta_{ij}\right) + C_5\rho k(b_{ik}\Omega_{jk} + b_{jk}\Omega_{ik}) \tag{8}$$

The mean strain-rate S_{ij}, the rotation tensor Ω_{ij}, the anisotropy tensor b_{ij}, the tensor invariant Π_{ij} and $\wp$ are expressed as

$$S_{ij} = \frac{1}{2}\left(\frac{\partial U_i}{\partial x_j} + \frac{\partial U_j}{\partial x_i}\right), \quad \Omega_{ij} = \frac{1}{2}\left(\frac{\partial U_i}{\partial x_j} - \frac{\partial U_j}{\partial x_i}\right)$$
$$\wp = -\overline{u_i u_j}\frac{\partial U_i}{\partial x_j}, \quad b_{ij} = \frac{\overline{u_i u_j} - \frac{2}{3}k\delta_{ij}}{2k}, \quad \Pi = b_{ij}b_{ji} \tag{9}$$

The constants $C_1 = 3.4$ and $C_2 = 4.2$ in this model are based upon realizability, dynamical systems considerations, and phase space portrait of return to isotropy experiments. However, $C_1^* = 1.80$, $C_3^* = 1.30$, $C_4 = 1.25$ and $C_5 = 0.40$ are obtained by numerical optimization. Rapid distortion theory (RDT) gave $C_3 = 0.8$, see Reference [3].

A simple Eddy viscosity (SEV) model based on the Boussinesq approximation calculates the third-order diffusion correlation

$$C_{ijk} = -\frac{\mu_\tau}{\sigma_c}\frac{\partial\overline{u_i u_j}}{\partial x_k}, \quad \sigma_c = 1 \tag{10}$$

Now it is evident that the RSM model can include the history-dependent non-local effects of the flow through convection and viscous diffusion of the Reynolds stresses. Further, these models can also qualitatively respond to streamline curvature, system rotation and stratification since they contain convection, production and body force. Moreover, the RSM model gives no reason for the normal stresses to be equal even if the mean strain rate vanishes.

3.2. Non-linear Eddy viscosity model (NLEVM)

A non-linear constitutive relation for the eddy viscosity in incompressible flow proposed by Speziale [16] is also considered in this investigation. The non-linear terms in this model are a form of quadratic terms, which enable calculation of anisotropic normal stresses and consequently prediction of the secondary velocity field in ducts. The Reynolds stresses in this model are determined according to

$$\rho\overline{u_i u_j} = \frac{2}{3}\rho k\delta_{ij} - 2\mu_\tau S_{ij} - 4C_D C_\mu\mu_\tau\frac{k}{\varepsilon}\left(S_{ik}S_{kj} - \frac{1}{3}S_{mn}S_{nm}\delta_{ij}\right) - 4C_E C_\mu\mu_\tau\frac{k}{\varepsilon}\left(\dot{S}_{ij} - \frac{1}{3}\dot{S}_{mm}\delta_{ij}\right) \tag{11}$$

and $\dot{S}_{ij}$ is the frame-indifferent Oldroyd derivative of S_{ij}, expressed as

$$\dot{S}_{ij} = \frac{\partial S_{ij}}{\partial t} + U_k \frac{\partial S_{ij}}{\partial x_k} - \frac{\partial U_i}{\partial x_k} S_{kj} - \frac{\partial U_j}{\partial x_k} S_{ki} \tag{12}$$

In Equation (11), $C_D = C_E = 1.68$.

Three key-criteria that guarantee consistency with certain properties of the exact Navier–Stokes equation are satisfied by this model; general co-ordinate and dimensional invariance, limited form of realizability and material frame indifference in the limit of two-dimensional turbulence (see Reference [12]).

3.3. Turbulence models for heat fluxes

Three models are used to express the turbulent heat fluxes.

(a) Simple Eddy diffusivity (SED) based on the Boussinesq viscosity model as

$$\rho\overline{u_j t} = -\frac{\mu_\tau}{\sigma_T} \frac{\partial T}{\partial x_j} \tag{13}$$

This model is the most common one in commercial codes. The main drawback of it is that the diffusivity is independent of the direction, i.e. isotropic. As an effect the temperature field contours have a similar shape as the main flow contours in duct flows, whether the main flow contours are wrongly or correctly predicted (dependent on the main flow contours).

(b) The Generalized gradient diffusion hypothesis (GGDH) expressed by Daly and Harlow [13],

$$\rho\overline{u_j t} = -\rho C_t \frac{k}{\varepsilon} \left(\overline{u_j u_k} \frac{\partial T}{\partial x_k} \right) \tag{14}$$

(c) Wealth α earnings $\times$ time (WET) given by Launder [14].

$$\rho\overline{u_j t} = -\rho C_t \frac{k}{\varepsilon} \left(\overline{u_j u_k} \frac{\partial T}{\partial x_k} + \overline{u_k t} \frac{\partial U_j}{\partial x_k} + \overline{f_j t} \right) \tag{15}$$

where $\overline{f_j t}$ is the buoyancy-driven heat flux and is zero in this case.

The constant C_t is set to 0.3 in both GGDH and WET. The advantages of the two last models are that they take into account the anisotropic behaviour of the heat transport in duct flows, independent on the main flow contours. However, these two models demand second order accuracy for the shear stresses. For example, they cannot generally be used with the LEVM in duct flows. Sometimes they may provide convergence problem in very complicated duct flows.

3.4. Equations for kinetic energy and its dissipation

From the above equations it is evident that the equations for the turbulent kinetic energy and its dissipation should also be solved. The transport equation for the kinetic energy and its dissipation are calculated by

$$\frac{\partial}{\partial t}(\rho k) + \frac{\partial}{\partial x_j}(\rho U_j k) = \frac{\partial}{\partial x_j} \left[\left(\mu + \frac{\mu_\tau}{\sigma_k} \right) \frac{\partial k}{\partial x_j} \right] + P_k - \rho\varepsilon \tag{16}$$

$$\frac{\partial}{\partial t}(\rho\varepsilon)+\frac{\partial}{\partial x_j}(\rho U_j\varepsilon)=\frac{\partial}{\partial x_j}\left[\left(\mu+\frac{\mu_\tau}{\sigma_\varepsilon}\right)\frac{\partial\varepsilon}{\partial x_j}\right]+C_{\varepsilon1}\frac{\varepsilon}{k}P_k-C_{\varepsilon2}\rho\frac{\varepsilon^2}{k} \tag{17}$$

where $\sigma_k=1.0$, $\sigma_\varepsilon=1.314$, $C_{\varepsilon1}=1.44$ and $C_{\varepsilon2}=1.83$. The term P_k is the production term expressed as

$$P_k=-\rho\overline{u_iu_j}\frac{\partial U_i}{\partial x_j} \tag{18}$$

The turbulent eddy viscosity μ_τ is calculated as

$$\mu_\tau=\rho C_\mu\frac{k^2}{\varepsilon},\quad C_\mu=0.09 \tag{19}$$

It should be noted that if RSM is used for the calculations then the equation for the kinetic energy could be solved in two ways:

(1) Solve for all the Reynolds stresses and let $k=0.5(\overline{uu}+\overline{vv}+\overline{ww})$
(2) Solve for kinetic energy and let one of the normal stresses (e.g. $\overline{uu}$) be set to

$$\overline{uu}=2k-(\overline{vv}+\overline{ww})$$

3.5. Periodic conditions

The pressure P is handled as

$$P(x,y,z)=-\beta x+P^*(x,y,z) \tag{20}$$

where β is a constant representing the non-periodic pressure gradient and P^* behaves in a periodic manner from cycle to cycle in the flow direction.

The dimensionless temperature θ is defined in the cyclic case as

$$\theta(x,y,z)=\frac{T(x,y,z)-T_\mathrm{w}}{T_\mathrm{b}(x)-T_\mathrm{w}} \tag{21}$$

where T_w is the constant wall temperature and T_b is the fluid bulk temperature. Using this expression and inserting it into the energy equation (3) one obtains in the steady state

$$\frac{\partial}{\partial x_j}(\rho U_j\theta)=\frac{\partial}{\partial x_j}\left[\frac{\mu}{Pr}\frac{\partial\theta}{\partial x_j}\right]+\frac{\partial}{\partial x_j}(-\rho\overline{u_j\theta})+\Omega \tag{22}$$

where Ω is

$$\Omega=\lambda\left[\Gamma\frac{\partial\theta}{\partial x}+\frac{\partial}{\partial x}(\Gamma\theta)-\rho U\theta\right]+\Gamma\theta\left(\lambda^2+\frac{\partial\lambda}{\partial x}\right) \tag{23}$$

and

$$\rho\overline{u_j\theta}=\frac{\rho\overline{u_jt}}{T_\mathrm{b}-T_\mathrm{w}} \tag{24}$$

In Equation (24) λ is

$$\lambda = \frac{\partial(T_b - T_w)}{\partial x} \Big/ (T_b - T_w) \tag{25}$$

The diffusion coefficient Γ is $\Gamma = \mu/Pr$. The parameters λ and Ω behave periodically.

In the GGDH method, $\overline{u_j t}$ is calculated from

$$\overline{u_j t} = -C_t \frac{k}{\varepsilon}(T_b - T_w)\left\{\overline{u_j u}\left(\lambda\theta + \frac{\partial\theta}{\partial x}\right) + \overline{u_j v}\frac{\partial\theta}{\partial y} + \overline{u_j w}\frac{\partial\theta}{\partial z}\right\} \tag{26}$$

In the WET method $\overline{u_j t}$, is determined from

$$\overline{u_j t} = -C_t \frac{k}{\varepsilon}(T_b - T_w)\left\{\overline{u_j u}\left(\lambda\theta + \frac{\partial\theta}{\partial x}\right) + \overline{u_j v}\frac{\partial\theta}{\partial y} + \overline{u_j w}\frac{\partial\theta}{\partial z} + \overline{u_k t}\frac{\partial U_j}{\partial x_k}\right\} \tag{27}$$

An additional condition is needed to close the problem since the energy equation contains two unknowns $\theta(x, y, z)$ and $\lambda(x)$. This condition can be obtained from the definition of the bulk temperature. In dimensionless form one has

$$\int |U|\theta \, dA_c = \int |U| \, dA_c \tag{28}$$

where A_c is the cross-sectional area perpendicular to the main flow direction. The shape of the non-dimensional temperature profile $\theta(x, y, z)$ repeats itself in the fully developed periodic region.

3.6. Boundary conditions

Periodicity conditions are imposed at the inlet and outlet for all variables. It then follows

$$\Phi(x, y, z) = \Phi(x + L, y, z)$$
$$\Phi = U, V, W, P^*, k, \varepsilon, \theta, \overline{u_i u_j} \tag{29}$$

In order to achieve numerical stability, the following variables are also handled as periodic: $\overline{u_j\theta}, \lambda, S_{ij}$.

3.7. Wall functions for momentum equations

The dissipation equation given in Equation (17) is valid for high Reynolds number only. Of course, it is possible to use damping functions in the dissipation equation and bridge it to a solid boundary. However, such damping functions need the wall-normal distance to a solid boundary which is not the subject of this study. Therefore, wall function treatment is used for the momentum equations. Furthermore, additional studies are needed to confirm how to remove the damping functions from the dissipation equation and still bridge it to a solid wall without using wall functions. Because, the dissipation equation has no natural boundary condition, it would be extremely difficult.

The law of the wall is assumed to be valid for both the flow and temperature fields in the near wall region. It is assumed that the region near the walls consists of only two layers, the viscous sublayer in which the turbulent viscosity is much smaller than the molecular viscosity and the log layer in which the turbulent viscosity is much greater than the molecular viscosity. The buffer layer is ignored. The traditional law of the wall is defined as

$$U^+ = \frac{U}{U^*} \cong \frac{1}{\kappa} \ln\ y^+ + B = \frac{1}{\kappa} \ln(Ey^+) \tag{30}$$

where

$$y^+ = \frac{\rho U^* \eta}{\mu} \tag{31}$$

and η is the distance normal to the wall. The von Karman constant is $\kappa = 0.4$ while the value of E for a smooth wall is $E = 9.8$.

The point $y^+ = 11.90$ is used to dispose the intersection (transition) between the viscous sublayer and log layer. Below this point the flow is assumed to be purely viscous (i.e. the turbulent stresses are negligible), and above this point the flow is assumed to be purely turbulent. The details can be found in Reference [4].

3.8. Wall functions for temperature equation

A similar treatment is applied to the temperature equation at the grid point adjacent to a wall. The heat flux close to the wall is assumed to be constant. The law of the wall for the temperature field is defined as

$$T^+ = \frac{(T_\mathrm{w} - T_\mathrm{p})\rho c_p U^*}{q_\mathrm{w}} = \frac{1}{\kappa_t} \ln\ y^+ + B_t \tag{32}$$

where $\kappa_t = 0.46$ suggested by Launder [14] is used here. For a cold wall and a medium with $Pr = 0.72$, the value of B_t is $B_t = 2.0$, see Reference [15]. The point $T^+ = 5.83$ is used here to dispose the intersection between the sublayer and the log layer. The transport equation reduces to:

$$q = (\Gamma_\mathrm{l} + \Gamma_\tau) c_p \frac{\partial T}{\partial \eta} = q_\mathrm{w} \tag{33}$$

(a) if $T^+ \geqslant 5.83$ where $\Gamma_\tau / \Gamma_\mathrm{l} \gg 1$, $q \cong q_\mathrm{w}$

The transport of heat is assumed to be entirely due to turbulence. q_w is calculated by using the following relation

$$\frac{q_\mathrm{w}}{c_p} = \frac{\rho U^* (T_\mathrm{w} - T_\mathrm{p})}{T^+} \tag{34}$$

(b) if $T^+ \leqslant 5.83$ where $\Gamma_\tau / \Gamma_\mathrm{l} \ll 1$, $q \cong q_\mathrm{w}$

The transport of heat is then assumed to be only due to molecular activity. q_w is calculated by using the following relation:

$$\frac{q_\mathrm{w}}{c_p} = \frac{\mu}{\eta Pr} (T_\mathrm{w} - T_\mathrm{p}) \tag{35}$$

3.9. Near wall treatment of the Reynolds stresses

The Reynolds stresses are set in a local stream aligned with a co-ordinate system with $\mathbf{n}=(n_x,n_y,n_z)$ and $\mathbf{t}=(t_x,t_y,t_z)$ as base unit vectors. $\mathbf{n}$ is the unit wall normal vector and $\mathbf{t}$ is the unit wall tangential vector and is aligned with the flow. The cross product of these vectors gives the third component in this orthogonal set. A simple co-ordinate transformation will then give the following stresses at the point adjacent to a wall, see Reference [16]:

$$\begin{aligned}
\overline{uu} &= t_x^2(\overline{uu})' + n_x^2(\overline{vv})' + 2t_xn_x(\overline{uv})' \\
&\quad + t_y^2n_z^2(\overline{ww})' - 2t_yn_zt_zn_y(\overline{ww})' + t_z^2n_y^2(\overline{ww})' \\
\overline{vv} &= t_y^2(\overline{uu})' + n_y^2(\overline{vv})' + 2t_yn_y(\overline{uv})' \\
&\quad + t_z^2n_z^2(\overline{ww})' - 2t_zn_xt_xn_z(\overline{ww})' + t_x^2n_z^2(\overline{ww})' \\
\overline{ww} &= t_z^2(\overline{uu})' + n_z^2(\overline{vv})' + 2t_zn_z(\overline{uv})' \\
&\quad + t_x^2n_y^2(\overline{ww})' - 2t_xn_yt_yn_x(\overline{ww})' + t_y^2n_x^2(\overline{ww})' \\
\overline{uv} &= t_xt_y(\overline{uu})' + (t_xn_y + t_yn_x)(\overline{uv})' + n_xn_y(\overline{vv})' \\
&\quad + t_xn_z(t_zn_y - t_yn_x)(\overline{ww})' + t_zn_x(t_yn_z - t_zn_y)(\overline{ww})' \\
\overline{vw} &= t_yt_z(\overline{uu})' + (t_yn_z + t_zn_y)(\overline{uv})' + n_yn_z(\overline{vv})' \\
&\quad + t_xn_y(t_zn_x - t_xn_z)(\overline{ww})' + t_yn_x(t_xn_z - t_zn_x)(\overline{ww})' \\
\overline{wu} &= t_zt_x(\overline{uu})' + (t_zn_z + t_xn_z)(\overline{uv})' + n_zn_z(\overline{vv})' \\
&\quad + t_yn_z(t_xn_y - t_yn_z)(\overline{ww})' + t_zn_z(t_yn_x - t_xn_y)(\overline{ww})'
\end{aligned} \tag{36}$$

At the node adjacent to a wall the dissipation rate is set to $\varepsilon = U_*^3/(k\eta_{\text{wall}})$ and the stresses are set as $(\overline{uu})' = 1.098k$, $(\overline{vv})' = 0.247k$ and $(\overline{uv})' = -0.255k$ (see, e.g. Reference [7]) where $k = U_*^2/\sqrt{C_\mu}$. U_* is computed from the wall functions.

3.10. Additional equations

Some additional equations have been used to calculate the Reynolds number, mass flow, the bulk velocity, pressure drop, Fanning friction factor and Nusselt number. The details of such a calculation procedure can be found in Reference [4]. Experiments carried out by Lowdermilk *et al.* [17] showed that the *Nu*-number in square ducts can be correlated with the Dittus–Boelter correlation (for about $Re \geqslant 8000$) and the friction factor can be correlated with the Prandtl friction law.

The calculated friction factor is thus compared with the Prandtl friction law (see Reference [18]) as

$$\frac{1}{\sqrt{4f}} = 2\,\log(Re\sqrt{4f}) - 0.8 \tag{37}$$

The *Re*-number is based on the hydraulic diameter

$$3\ \text{Walls} \Rightarrow D_{\text{h}} = \frac{4A_{\text{cross}}}{a + b + \dfrac{h}{\sin\varphi}} \quad \text{(trapezoidal)}$$

$$2\ \text{Walls} \Rightarrow D_{\text{h}} = \frac{4A_{\text{cross}}}{a + \dfrac{h}{\sin\varphi}} \quad \text{(square, rectangular)} \tag{38}$$

where a, b, h and φ are base-length, upper-length, height and base-angle, respectively.

The *Nu*-number is calculated in two ways: (1) by calculating the local *Nu*-number at each point adjacent to a wall and then integrate these over all the walls (Nu_x), (2) by using the periodic conditions and calculate the overall *Nu*-number by a heat balance equation (Nu_{ov}). These are called local and overall *Nu*-numbers, respectively. The details of this procedure can also be found in Reference [19]. The calculated *Nu*-numbers are compared with the Dittus–Boelter correlation (see Reference [18]) as

$$Nu = 0.023Re^{0.8}Pr^{0.3} \quad \text{for } Re \geqslant 8000 \tag{39}$$

The *Nu* values calculated by these two methods should ideally be very close to each other. If not, something is not properly considered, for example the y^+ value near the walls. The differences between these two calculated *Nu*-numbers are less than 1% for all cases considered in this study.

4. NUMERICAL SOLUTION PROCEDURE

The partial differential equations are transformed to algebraic equations by a general finite-volume technique. The momentum equations are solved for the velocity components on a non-staggered grid arrangement. The Rhie–Chow interpolation method [20] is used to interpolate the velocity components to the control volume faces from the grid points. The SIMPLEC-algorithm is employed to handle the pressure velocity coupling. A modified strongly implicit procedure (SIP) algorithm is used for solving the equations. The convective terms are treated by the QUICK scheme while the diffusive terms are treated by the central-difference scheme. The hybrid scheme is used for solving the k and ε equations.

A non-uniform grid distribution is employed in the plane perpendicular to the main flow direction. Close to each wall, the number of grid points or control volumes is increased to enhance the resolution and accuracy. The Prandtl number was set to 0.72 and the computations were terminated when the sum of the absolute residuals normalized by the inflow was less than 10^{-4} for all variables with the RSM model and less than 10^{-5} with the non-linear model.

It should be noted that the average y^+-value adjacent to a wall is between 40 and 44 in all the calculations. This has been secured in the calculations since it is well known that the results obtained with wall functions are dependent on the y^+-value and the best results may be obtained when the y^+-value at the point adjacent to a wall is larger than about 35. A more complete discussion about the y^+-value at the point adjacent to a wall can be

found in Reference [4]. Different set of grid arrangement is used to ensure that the results are independent of the number grids and grid arrangement.

The calculations showed that the SSG model is only weekly dependent on the y^+-value near the walls.

5. RESULTS AND DISCUSSIONS

5.1. Square ducts

The predicted secondary velocity field using the SSG model compared with the non-linear k–ε model is shown in Figure 2. The non-linear model predicts the secondary motion very well and almost in consistent with the RSM model. A comprehensive comparison between the predicted secondary motions and experimental results, direct numerical simulation and large Eddy simulation can be found in Reference [4].

Table I shows the calculated Fanning friction factor and *Nu*-number in comparison with the existing correlations, for two different *Re*-numbers. Excellent agreement between the calculations and the correlations has been obtained for the friction factor and the *Nu*-number if the heat fluxes are calculated by the GGDH and the WET methods. However, the SED model deviates somewhat from the Dittus–Boelter correlation.

Figure 3 shows the streamwise velocity contours predicted by the SSG model compared with the non-linear k–ε model. In the region close to the corner, the contours are bulged towards the corner due to the presence of the secondary motions. As can be seen from Figure 3, the non-linear k–ε model shows less bulging towards the corner which means that the secondary motions are somewhat underestimated. To reveal how the bulging affects the prediction of the

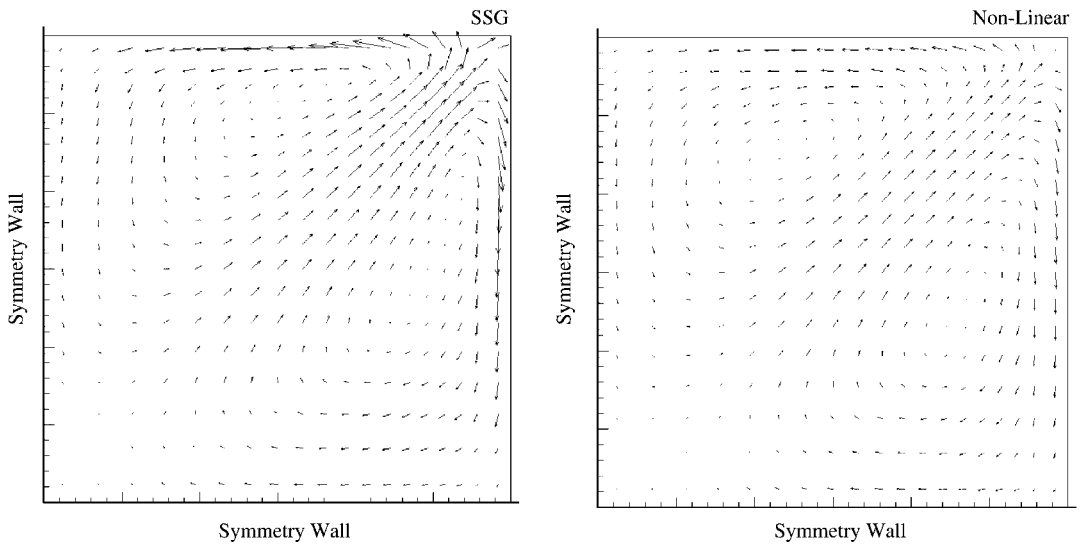

Figure 2. Secondary velocity field predicted by the RSM and the non-linear k–ε model. $Re = 33472$.

Table I. Calculated *Nu*-numbers and Fanning friction factors by the RSM (SSG) model compared with the Dittus–Boelter and Prandtl friction law correlations in a square duct.

Model	*Re*	*Nu*	Nu_{DB}	Diff%	$f \times 10^3$	$f_{Pra} \times 10^3$	Diff%
SED	23261.9	58.3	64.9	10.2	6.374	6.238	−2.2
GGDH	”	65.0	64.9	0.0	6.374	6.238	−2.2
WET	”	64.8	64.9	0.2	6.374	6.238	−2.2
SED	33472.0	76.7	86.8	11.7	5.598	5.723	2.2
GGDH	”	85.9	86.8	1.1	5.598	5.723	2.2
WET	”	85.6	86.8	1.4	5.598	5.723	2.2

Diff = 100 × (correlated − calculated)/correlated.

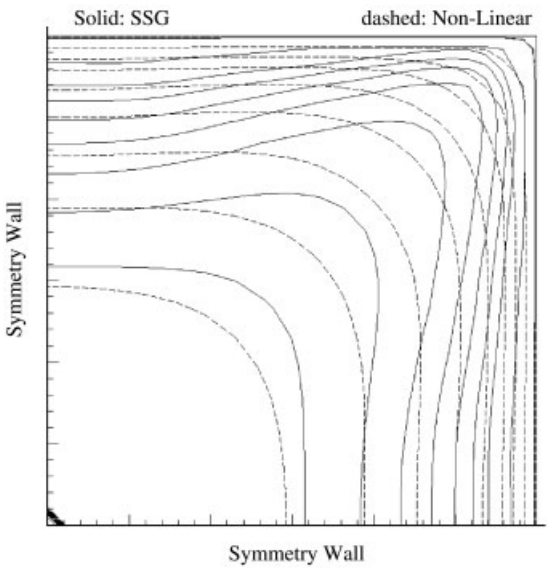

Figure 3. Streamwise velocity contours. *Re* = 33472.

friction factor and the *Nu*-number, Table II is presented. As can be seen from the table the affect of these bulging on the overall properties, *Nu*-number and friction factor are small and negligible.

As shown in Table II, the friction factors and the *Nu*-numbers predicted by the non-linear k–ε model also agree reasonably with the correlation. However, the non-linear model converges much faster and the residuals can be smaller than for the RSM model.

5.2. *Trapezoidal ducts*

Figure 4 shows the predicted secondary velocity motions in a trapezoidal duct using the RSM model and the non-linear k–ε model. Even here, the non-linear model predicts the secondary motions similar to the RSM model. However, the secondary motions are somewhat

Table II. Calculated *Nu*-numbers and friction factors by the RSM (SSG) model compared with the non-linear k–ε model of Speziale and the correlations in a square duct.

Model	*Re*	*Nu*	Diff%	$f_{\mathrm{Pra}} \times 10^3$	Diff%
RSM + (GGDH)	23261.9	65.0	0.0	6.238	−2.2
Non-linear + (GGDH)	23839.9	59.6	9.9	6.632	−6.9
RSM + (GGDH)	33472.0	85.9	1.1	5.598	2.2
Non-linear + (GGDH)	33543.2	78.7	9.6	6.131	−7.2

Diff = 100 × (correlated − calculated)/correlated.

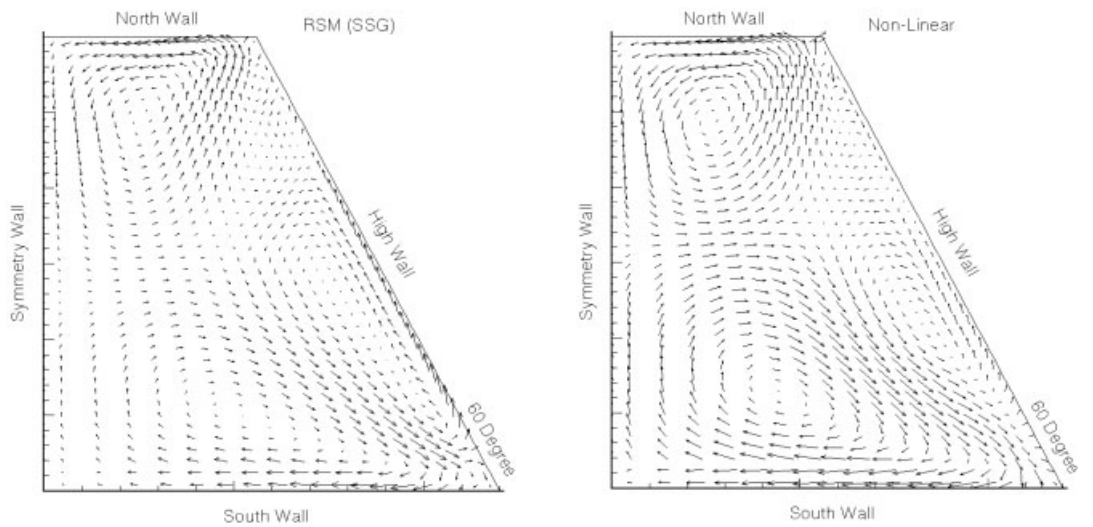

Figure 4. Predicted secondary motions by the RSM model as well as the non-linear model k–ε model in a trapezoidal duct.

underestimated by the non-linear model, see Figure 5. Therefore, the bulging towards the corners is less evident in the non-linear model than in the RSM model. This is so, because the temperature field is strongly dependent on the prediction of the main flow, the bulging near the corner of the temperature field will also be less evident for the non-linear case than for the RSM case (not shown here).

In addition, the calculation time by the RSM model is about twice that of the non-linear model in this case as well as in previous cases.

6. CONCLUSIONS

A full Reynolds stress model (RSM) and heat transfer model have been successfully applied for numerical investigation of turbulent flow in straight ducts. The non-linear eddy viscosity model of Speziale was found to underestimate the secondary flow compared to the RSM. The

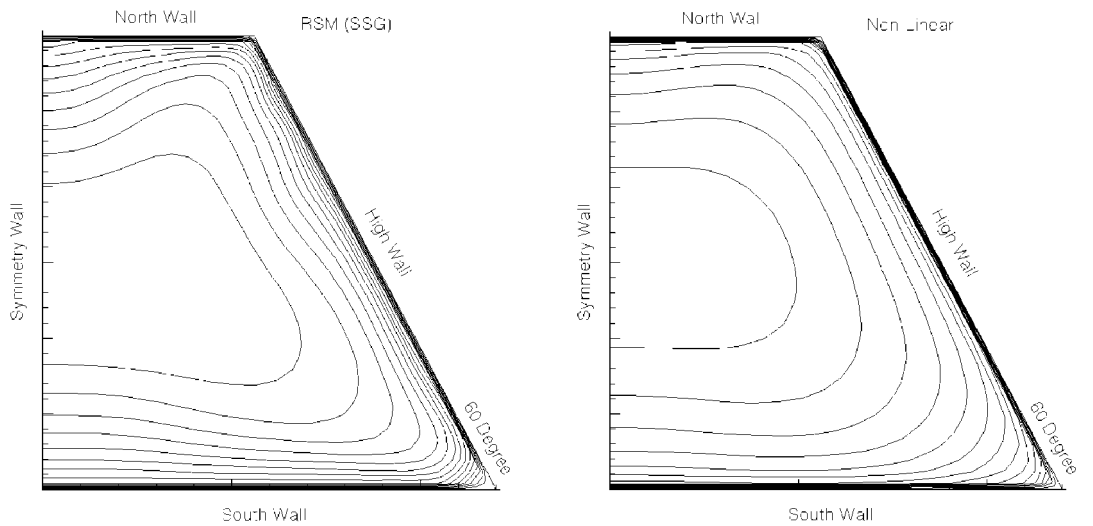

Figure 5. Streamwise velocity contours in a trapezoidal duct using the RSM model and the non-linear model k–ε model.

turbulent heat fluxes are modelled with SED, GGDH and WET methods (the latter two provide the most accurate results). Wall functions for the momentum equations and the temperature fields are employed, separately, and Jayatilleke's P-function is abandon.

The average friction factors predicted by the RSM model agree excellent with the Prandtl friction law correlation. The calculated Nu-numbers obtained by the GGDH and WET concepts are in good agreement with the Dittus–Boelter correlation. However, the SED underestimates the Nusselt numbers compared to this correlation.

One important conclusion of this investigation is that the non-linear eddy viscosity model is able to predict the friction factor and the Nu-number is in decent agreement with the RSM model but with considerably less computational effort and time. Moreover, the secondary motions predicted by the non-linear model is very similar to the one predicted by the RSM model.

REFERENCES

1. Hanjaliç K. Advanced turbulence closure models: a review of current status and future prospects. *International Journal of Heat and Fluid Flow* 1994; **15**(3):178–203.
2. Launder BE, Li SP. On the elimination of the wall topography parameters from second-moment closure. *Physics of Fluids* 1993; **6**(2):999–1006.
3. Speziale CG, Sarkar S, Gatski TB. Modelling the pressure-strain correlation of turbulence: an invariant dynamical systems approach. *Journal of Fluid Mechanics* 1991; **227**:245–272.
4. Rokni M, Sundén B. A numerical investigation of turbulent forced convection in ducts with rectangular and trapezoidal cross-section area by using different turbulence models. *Numerical Heat Transfer* 1996; **30**(4): 321–346.
5. Rokni M, Sundén B. 3D Numerical investigation of turbulent forced convection in wavy ducts with trapezoidal cross section. *Numerical Methods for Heat and Fluid Flow* 1998; **8**(1):118–141.
6. Demuren AO, Rodi W. Calculation of turbulence-driven secondary motion in non-circular ducts. *Journal of Fluid Mechanics* 1984; **140**:189–222.
7. Launder BE, Reece GL, Rodi W. Progress in the development of a Reynolds-stress turbulence closure. *Journal of Fluid Mechanics* 1975; **68**(3):537–566.

8. Mompean G, Gavrilakis S, Machiels L, Deville MO. On predicting the turbulence-induced secondary flows using non-linear $k-\varepsilon$ models. *Physics of Fluids* 1996; **8**(7):1856–1868.
9. Naimi M, Gessner, FB. A calculation method for developing turbulent flow in rectangular ducts of arbitrary aspect ratio. *Journal of Fluids Engineering* (*ASME*) 1995; **117**:249–258.
10. Myong HK, Kobayashi T. Prediction of three-dimensional developing turbulent flow in a square duct with an anisotropic low-Reynolds number $k-\varepsilon$ model. *Journal of Fluids Engineering* (*ASME*) 1991; **113**:608–615.
11. Speziale CG. On non-linear K-l and K-ε models of turbulence. *Journal of Fluid Mechanics* 1987; **178**: 459–475.
12. Speziale CG. Some interesting properties of two-dimensional turbulence. *Physics of Fluids* 1981; **24**(8): 1425–1427.
13. Daly BJ, Harlow FH. Transport equations in turbulence. *Physics of Fluids* 1970; **13**:2634–2649.
14. Launder BE. On the computation of convective heat transfer in complex turbulent flows. *ASME Journal of Heat Transfer* 1988; **110**:1112–1128.
15. Mohammadi B, Pironneau O. *Analysis of the K-Epsilon Turbulence Model*. Wiley: New York, 1993.
16. Perzon S, Davidson L, Ramnefors M. Reynolds stress modelling of complex flows over curved surfaces. In *Flow Modelling and Turbulence Measurements VI*, Chen CJ, Shih C, Lineau J, King RJ (Eds), A.A. Balkema: Rutherdam, 1996; 407–414.
17. Lowdermilk WH, Wieland WF, Livingood JNB. Measurements of heat transfer and friction coefficients for flow of air in noncircular ducts at high surface temperature. *NACA RN E53J07*, 1954.
18. Incropera FP, DeWitt DP. *Fundamentals of Heat and Mass Transfer* (4th edn). Wiley: New York, 1996.
19. Rokni M, Sundén B. Performance of RNG turbulence modelling for turbulent forced convective heat transfer in ducts. *International Journal of CFD* 1997; **11**:351–362.
20. Rhie CM, Chow WL. Numerical study of the turbulent flow past an airfoil with trailing edge separation. *AIAA Journal* 1983; **21**(11):1525–1532.

